

NUMERICAL SOLUTION OF AN UNSTEADY MHD FLOW OF A ROTATING FLUID PAST AN INFINITE VERTICAL POROUS PLATE IN THE PRESENCE OF RADIATION AND CHEMICAL REACTION

K. ANITHA

ABSTRACT. Finite element solution of an unsteady hydromagnetic natural convection heat and mass transfer flow of a rotating, incompressible, viscous Boussinesq fluid is presented in this study in the presence of radiative heat transfer and a first order chemical reaction between the fluid and the diffusing species. The Rosseland approximation for an optically thick fluid is invoked to describe the radiative flux. Results obtained show that a decrease in the temperature boundary layer occurs when the Prandtl number and the radiation parameter are increased and the flow velocity approaches steady state as the time parameter is increased. These findings are in quantitative agreement with earlier reported studies.

1. INTRODUCTION

The phenomenon of free convection arises in the fluid when temperature changes cause density variation leading to buoyancy forces acting on the fluid elements. Considerable attention has been given to the unsteady free convection flow of viscous incompressible, electrically conducting fluid in presence of applied magnetic field in connection with the theories of fluid motion in the liquid core of the Earth and also meteorological and oceanographic applications. It is worth mentioning that MHD is now undergoing a stage of great enlargement and differentiation of subject matter. These new problems draw the attention of the researchers due to their varied significance, in liquid metals, electrolytes and ionized gases etc. In geophysics, it finds its applications in the design of MHD generators and accelerators, underground water energy storage system etc. It is worth mentioning that MHD is now undergoing a stage of great enlargement and differentiation of subject matter. The flow of an incompressible Boussinesq fluid in the presence of rotation has applications in space science and engineering fluid dynamics. Bestman and Adjepong [3] studied the unsteady hydro magnetic free convection flow with radiative heat transfer in

2010 *Mathematics Subject Classification.* 80A20, 65M60, 80A20.

Key words and phrases. MHD, Chemical reaction, Natural convection, Rotating fluid, Radiative heat transfer, Optically thick fluid, Radiation, Finite element method.

Submitted August 2, 2014. Revised August 27, 2014 .

a rotating fluid. Free convection heat transfer to steady radiating non Newtonian MHD flow past a vertical porous plate was studied by Bestman [4]. Azzam [2] investigated the effect of Radiation on the MHD mixed free fixed convective flow past a semi infinite moving vertical plate for high temperature differences. Elbarbary et al.[8] investigated finite difference method for the effect of variable viscosity on magneto micro polar fluid flow with radiation. Helmy[9] studied an Unsteady free convection flow past a vertical porous plate. Unsteady magnetohydrodynamic micro polar fluid flow and heat transfer over a vertical porous medium in the presence of thermal and mass diffusion with constant heat source was studied by Ibrahim[10]. Jha [11] studied MHD free convection and mass transfer flow through a porous medium but did not consider the effect of radiation which is of great relevance to astrophysical and cosmic studies. Effects of chemical reaction, heat and mass transfer along a wedge with heat source and concentration in the presence of suction or injection was explored by Kandaswamy[12]. The effects of Hall current on hydromagnetic free convection with mass transfer in a rotating fluid was studied by Agrawal et al. [1]. Recently, Chamkha [5] investigated unsteady convective heat and mass transfer past a semi infinite permeable moving plate with heat absorption where it was found that increase in solutal Grashof number enhanced the concentration buoyancy effects leading to an increase in the velocity. In other recent study Ibrahim et al. [11] investigated unsteady magnetohydrodynamic micro polar fluid flow and heat transfer over a vertical porous plate through a porous medium in the presence of thermal and mass diffusion with a constant heat source. Chamkha and Cookey [6],[7], give a good review on MHD flows through a porous medium. Ogulu[14] investigated on MHD free convection and mass transfer flow with radiative heat transfer. Singh et al. [15] Studied the Finite difference analysis of unsteady hydromagnetic free convection flow with constant heat flux. Motivated by the work above, objective of the present work is to study the effects of Chemical reaction on an unsteady magnetohydrodynamic flow of a rotating fluid past a vertical porous plate in the presence of radiation. Hence, the purpose of this study is to extend Muthucumaraswamy and Ganesan [13] to study the unsteady problem which includes internal thermal radiation and chemical reaction for first order. The governing equations are solved numerically using a very efficient finite element method known as Galerkin method. The results obtained under special cases are then compared with those of Muthucumaraswamy and Ganesan [13] in absence of thermal radiation by using Laplace transform technique and found to agree very favorably. In this study, the effects of different flow parameters encountered in the equations are also studied. The problem is solved numerically using the Galerkin finite element method, which is more economical from the computational view point.

2. MATHEMATICAL FORMULATION

We consider in three dimensions the unsteady motion of an incompressible electrically conducting viscous fluid which moves in its own plane with velocity U_0 and rotates with angular velocity Ω as in [4]. We assume a uniform magnetic field B_0 applied in the direction of the flow fixed relative to the plate. We also assume that induced magnetic fields are negligible in comparison with the applied field. Further, we assume no applied voltage present which means no electric field present

and viscous dissipation heating is absent in the energy equation. With these assumptions and those usually associated with the Boussinesq approximations, the proposed governing equations are

$$\frac{\partial u'}{\partial t'} - 2\Omega'v' = v\frac{\partial^2 u'}{\partial t'^2} - \frac{\sigma B_0^2 u'}{\rho_\infty} - \frac{vu'}{K'} + g\beta(T - T_\infty) + g\beta^*(C' - C'_\infty) \quad (1)$$

$$\frac{\partial u'}{\partial t'} - 2\Omega'u' = v\frac{\partial^2 v'}{\partial t'^2} - \frac{\sigma B_0^2 v'}{\rho} - \frac{vv'}{K'} \quad (2)$$

$$\frac{\partial T}{\partial t'} = \frac{k}{\rho C_P} \left[\frac{\partial^2 T}{\partial y'^2} - \frac{1}{k} \frac{\partial q'_r}{\partial y'} \right] \quad (3)$$

$$\frac{\partial C'}{\partial t'} = D_m \frac{\partial^2 C'}{\partial y'^2} - k'_r(C' - C'_\infty) \quad (4)$$

Subject to the conditions

$$\begin{aligned} t' \leq 0 : u' = U_0, v' = 0, T = T_\infty, C' = C_\infty \text{ for all } y' \\ t' > 0 : \begin{cases} u' = U_0, v' = 0, T = T_w, C' = C_w & \text{at } y' = 0 \\ u' = U_0, v' = 0, T = T_\infty, C' = C_\infty & \text{as } y' \rightarrow \infty \end{cases} \end{aligned} \quad (5)$$

We now introduce the following non-dimensional quantities and parameters

$$\begin{aligned} t' = \frac{vt}{U_0^2}, y' = \frac{vy}{U_0}, u' = uU_0, v' = vU_0, K' = \frac{v^2 K}{U_0^2}, \Omega' = \frac{U_0^2 \Omega}{v}, \\ q'_r = \frac{U_0 k q_r}{\rho C_P}, S_c = \frac{v}{D_m}, P_r = \frac{\mu C_P}{k}, M^2 = \frac{\sigma v B_0^2}{\rho U_0^2}, G_r = \frac{g\beta v(T - T_\infty)}{U_0^3}, \\ G_c = \frac{g\beta^* v(C' - C'_\infty)}{U_0^3}, \theta = \frac{T - T_w}{T - T_\infty}, C = \frac{C' - C'_w}{C' - C'_\infty}, k_r = \frac{k'_r v}{U_0^2} \end{aligned} \quad (6)$$

Where u, v , Velocity components; q , Complex velocity; U_0 , Scale of free stream velocity; y , Coordinate; T , Dimensional temperature; C' , Dimensional species concentration; t , Time; k , Thermal conductivity; D_m , Solutal diffusivity; ρ , density; C_P , Specific heat at constant pressure; ϵ , Time corrective parameter; β , Coefficients of volume expansion due to temperature; β^* , Coefficient of volume expansion due to concentration; M^2 , Hartmann number; P_r , Prandtl number; S_c , Schmidt number; k_r , Chemical reaction constant; K , Porosity parameter; θ , nondimensional temperature; C , Nondimensional species concentration; g , Acceleration due to gravity; G_r , Grashof number; G_c , Modified Grashof number; σ , Electrical conductivity; v , Kinematic coefficient of viscosity; Ω , Angular velocity; B_0 , Magnetic field strength; q_r , Radiative flux vector; Subscripts: w , Wall condition; ∞ , Free stream condition.

Introducing equation (6) into equations (1)-(5) we obtain

$$\frac{\partial u}{\partial t} - 2\Omega v = \frac{\partial^2 u}{\partial y^2} - M^2 u - \frac{u}{K} + G_r \theta + G_c C \quad (7)$$

$$\frac{\partial v}{\partial t} - 2\Omega u = \frac{\partial^2 v}{\partial y^2} - M^2 v - \frac{v}{K} \quad (8)$$

$$\frac{\partial \theta}{\partial t} = \frac{1}{P_r} \left(\frac{\partial^2 \theta}{\partial y^2} - \frac{\partial q_r}{\partial y} \right) \quad (9)$$

$$\frac{\partial C}{\partial t} = \frac{1}{S_c} \frac{\partial^2 C}{\partial y^2} - k_r C \quad (10)$$

We now find it convenient to combine equations (1) and (2) into a single equation. We multiply equation (2) by i and add the resultant to equation (1) to obtain

$$\frac{\partial q}{\partial t} + \left(2i\Omega + M^2 + \frac{1}{K}\right) q = \frac{\partial^2 q}{\partial y^2} + G_r \theta + G_c C \quad (11)$$

$q = u + iv$ and $i = -1$

Further, for the radiative heat flux in equation (9) we invoke the differential approximation, Elbarbary and Elgazery [8]

$$\nabla \cdot q_r = 4(T - T_w) \int_0^\infty \alpha^2 \left(\frac{\partial \beta}{\partial T} \right) d\lambda \quad (12)$$

For an optically thick fluid, as noted in Azzam [2], in addition to emission there is also self absorption and usually the absorption coefficient is wavelength dependent and large (as noted in [4]) so we can adopt the Rosseland approximation of equation (12) where the radiative flux vector q_r is given by

$$q_r = -\frac{4\sigma^*}{3\alpha} \frac{\partial T^4}{\partial y} \quad (13)$$

Where σ^* - the Stefan-Boltzmann constant and α - the mean absorption coefficient. It should be noted that by using Rosseland approximation, the present analysis is limited to optically thick fluids. If temperature differences within the flow are sufficient, small, then equation (13) can be linearised by expanding T^4 in the Taylor series about T_∞ , which after neglecting higher order terms take the form

$$T^4 \cong 4T_\infty^3 T - 3T_\infty^4 \quad (14)$$

Substituting equation (14) into equation (9) we obtain

$$\frac{\partial \theta}{\partial t} = \left(\frac{1 + N}{Pr} \right) \frac{\partial^2 \theta}{\partial y^2} \quad (15)$$

Where $N = \frac{3\alpha k}{4\sigma^* T_\infty^3}$ is the radiation parameter.

The initial and boundary conditions are now

$$\begin{aligned} t \leq 0 : q(y, t) = \theta(y, t) = C(y, t) = 0 \\ t > 0 : \begin{cases} q(0, t) = q_0 \quad \theta(0, t) = 1 \quad C(0, t) = 1 \\ q(\infty, t) \rightarrow 0 \quad \theta(\infty, t) \rightarrow 0 \quad C(\infty, t) \rightarrow 0 \end{cases} \end{aligned} \quad (16)$$

The mathematical statement of the problem is now complete.

3. METHOD OF SOLUTION

By applying Galerkin finite element method for equation (11) over the element (e) , $(y_j \leq y \leq y_k)$ is

$$\int_{y_j}^{y_k} \left\{ N^{(e)T} \left[\frac{\partial^2 q^{(e)}}{\partial y^2} - \frac{\partial q^{(e)}}{\partial t} - Rq^{(e)} + P \right] \right\} dy = 0 \quad (17)$$

where $P = (G_r)\theta + (G_c)C$, $R = 2i\Omega + M^2 + \frac{1}{K}$

Integrating the first term in equation (17) by parts one obtains

$$N^{(e)T} \left\{ \frac{\partial q^{(e)}}{\partial y} \right\}_{y_j}^{y_k} - \int_{y_j}^{y_k} \left\{ \frac{\partial N^{(e)T}}{\partial y} \frac{\partial q^{(e)}}{\partial y} + N^{(e)T} \left[\frac{\partial q^{(e)}}{\partial t} - Rq^{(e)} + P \right] \right\} dy = 0 \quad (18)$$

Neglecting the first term in equation (18), one gets:

$$\int_{y_j}^{y_k} \left\{ \frac{\partial N^{(e)T}}{\partial y} \frac{\partial q^{(e)}}{\partial y} + N^{(e)T} \left[\frac{\partial q^{(e)}}{\partial t} - Rq^{(e)} + P \right] \right\} dy = 0$$

let $q^{(e)} = N^{(e)}\phi^{(e)}$ be the linear piecewise approximation solution over the element $(e)(y_j \leq y \leq y_k)$ where $N^{(e)} = [N_j \ N_k]$, $\phi^{(e)} = [u_j \ u_k]^T$, and $N_j = \frac{y_k - y}{y_k - y_j}$, $N_k = \frac{y - y_j}{y_k - y_j}$ are the basis functions. one obtains:

$$\int_{y_j}^{y_k} \left\{ \begin{bmatrix} N'_j N'_j & N'_j N'_k \\ N'_k N'_j & N'_k N'_k \end{bmatrix} \begin{bmatrix} q_j \\ q_k \end{bmatrix} \right\} dy + \int_{y_j}^{y_k} \left\{ \begin{bmatrix} N_j N_j & N_j N_k \\ N_k N_j & N_k N_k \end{bmatrix} \begin{bmatrix} \dot{q}_j \\ \dot{q}_k \end{bmatrix} \right\} dy + \\ R \int_{y_j}^{y_k} \left\{ \begin{bmatrix} N_j N_j & N_j N_k \\ N_k N_j & N_k N_k \end{bmatrix} \begin{bmatrix} q_j \\ q_k \end{bmatrix} \right\} dy = P \int_{y_j}^{y_k} \begin{bmatrix} N_j \\ N_k \end{bmatrix} dy$$

simplifying we get

$$\frac{1}{l^{(e)2}} \begin{bmatrix} 1 & -1 \\ -1 & 1 \end{bmatrix} \begin{bmatrix} q_j \\ q_k \end{bmatrix} + \frac{1}{6} \begin{bmatrix} 2 & 1 \\ 1 & 2 \end{bmatrix} \begin{bmatrix} \dot{q}_j \\ \dot{q}_k \end{bmatrix} + \frac{R}{6} \begin{bmatrix} 2 & 1 \\ 1 & 2 \end{bmatrix} \begin{bmatrix} q_j \\ q_k \end{bmatrix} = \frac{P}{2} \begin{bmatrix} 1 \\ 1 \end{bmatrix}$$

Where prime and dot denotes differentiation with respect to y and time t respectively. Assembling the element equations for two consecutive elements $(y_{i-1} \leq y \leq y_i)$ and $(y_i \leq y \leq y_{i+1})$ following is obtained:

$$\frac{1}{l^{(e)2}} \begin{bmatrix} 1 & -1 & 0 \\ -1 & 2 & -1 \\ 0 & -1 & 1 \end{bmatrix} \begin{bmatrix} q_{i-1} \\ q_i \\ q_{i+1} \end{bmatrix} + \frac{1}{6} \begin{bmatrix} 2 & 1 & 0 \\ 1 & 2 & 1 \\ 0 & 1 & 2 \end{bmatrix} \begin{bmatrix} \dot{q}_{i-1} \\ \dot{q}_i \\ \dot{q}_{i+1} \end{bmatrix} + \\ \frac{R}{6} \begin{bmatrix} 2 & 1 & 0 \\ 1 & 4 & 1 \\ 0 & 1 & 2 \end{bmatrix} \begin{bmatrix} q_{i-1} \\ q_i \\ q_{i+1} \end{bmatrix} = \frac{P}{2} \begin{bmatrix} 1 \\ 2 \\ 1 \end{bmatrix} \quad (19)$$

Now put row corresponding to the i to zero, from equation (19) the difference schemes with $l^{(e)} = h$ is:

$$\frac{1}{h^2} [-q_{i-1} + 2q_i - q_{i+1}] + \frac{1}{6} [\dot{q}_{i-1} + 4\dot{q}_i + \dot{q}_{i+1}] + \frac{R}{6} [q_{i-1} + 4q_i + q_{i+1}] = P \quad (20)$$

Applying the trapezoidal rule, following system of equations in Crank-Nicholson method are obtained:

$$A_1 q_{i-1}^{n+1} + A_2 q_i^{n+1} + A_3 q_{i+1}^{n+1} = A_4 q_{i-1}^n + A_5 q_i^n + A_6 q_{i+1}^n + P^* \quad (21)$$

Now from equations (10) and (15) following equations are obtained:

$$B_1 \theta_{i-1}^{n+1} + B_2 \theta_i^{n+1} + B_3 \theta_{i+1}^{n+1} = B_4 \theta_{i-1}^n + B_5 \theta_i^n + B_6 \theta_{i+1}^n \quad (22)$$

$$C_1 C_{i-1}^{n+1} + C_2 C_i^{n+1} + C_3 C_{i+1}^{n+1} = C_4 C_{i-1}^n + C_5 C_i^n + C_6 C_{i+1}^n \quad (23)$$

Where $A_1 = 2 - 6r + Rk$, $A_2 = 8 + 12r + 4Rk$, $A_3 = 2 - 6r + Rk$, $A_4 = 2 + 6r - Rk$, $A_5 = 8 - 12r - 4Rk$, $A_6 = 2 + 6r - Rk$

$B_1 = 2(Pr) - 6(1 + N)r$, $B_2 = 8(Pr) + 12(1 + N)r$, $B_3 = 2(Pr) - 6(1 + N)r$,

$B_4 = 2(Pr) + 6(1 + N)r$, $B_5 = 8(Pr) + 12(1 + N)r$, $B_6 = 2(Pr) + 6(1 + N)r$,

$C_1 = 2(Sc) - 6r + k_r(Sc)k$, $C_2 = 8(Sc) + 12r + 4k_r(Sc)k$, $C_3 = 2(Sc) - 6r + k_r(Sc)k$,

$C_4 = 2(Sc) + 6r - k_r(Sc)k$, $C_5 = 8(Sc) - 12r - 4k_r(Sc)k$, $C_6 = 2(Sc) + 6r - k_r(Sc)k$,

$P^* = 12phk = 12hk(Gr)\theta + 12hk(Gc)C$

Here $r = \frac{k}{h^2}$ and h, k are mesh sizes along y direction and time direction respectively.

Index i refers to space and j refers to the time. In the equations (21),(22) and (23), taking $i = 1(1)n$ and using boundary conditions (16), then the following system of equations are obtained:

$$A_i X_i = B_i, \quad i = i(1)3 \quad (24)$$

where A_i 's are matrices of order n and X_i, B_i 's are column matrices having n components. The solutions of above system of equations are obtained by using Thomas algorithm for velocity, temperature and concentration. Also, numerical solutions for these equations are obtained by C programme. In order to prove the convergence and stability of Galerkin finite element method, the same C programme was run with smaller values of h and k no significant change was observed in the values of q, θ and C Hence the Galerkin finite element method is stable and convergent.

Skin friction and Rate of heat transfer

The expression for skin friction coefficient (τ) at the plate is $\tau = \left(\frac{\partial q}{\partial y} \right)_{y=0}$ (25)

The rate of Heat transfer coefficient (Nu) at the plate is $Nu = - \left(\frac{\partial \theta}{\partial y} \right)_{y=0}$ (26)

The rate of Mass transfer coefficient (Sh) at the plate is $Sh = - \left(\frac{\partial C}{\partial y} \right)_{y=0}$ (27)

4. RESULTS AND DISCUSSION

The problem of radiative heat transfer to unsteady hydromagnetic flow involving heat and mass transfer is addressed in this study. Numerical calculations have been carried out for the non dimensional Temperature (θ), Concentration (C), Complex velocity (q) keeping the other parameters of the problem fixed. The solution obtained for the velocity is complex and only the real part of the complex quantity is invoked for the numerical discussion with the help of Abramowitz and Stegun [1]. Numerical calculations of these results are presented graphically in figures (1)-(10). These results show the effect of material parameters on the temperature distribution, concentration profiles, complex velocity and the shear stress at the wall. And the results of skinfriction (τ) due to complex velocity, Rate of heat transfer (Nu) due to temperature and mass transfer (Sh) due to concentration are presented in tabular form. To find out the solution of this problem, we have placed an infinite vertical plate in a finite length in the flow. Hence, we solve the entire problem in a finite boundary. However, in the graphs, the y values vary from 0 to 4 and the complex velocity, temperature, and concentration tend to zero as y tends to 4. This is true for any value of y . Thus, we have considered finite length.

The temperature and the species concentration are coupled to the velocity via Grashof number (Gr) and Modified Grashof number (Gc) as seen in equation (11). For various values of Grashof number and Modified Grashof number, the velocity profiles u are plotted in figures (1) and (2). The Grashof number (Gr) signifies the relative effect of the thermal buoyancy force to the viscous hydrodynamic force in the boundary layer. As expected, it is observed that there is a rise in the velocity due to the enhancement of thermal buoyancy force. Also, as (Gr) increases, the peak values of the velocity increases rapidly near the porous plate and then decays smoothly to the free stream velocity. The Modified Grashof number (Gc)

defines the ratio of the species buoyancy force to the viscous hydrodynamic force. As expected, the fluid velocity increases and the peak value is more distinctive due to increase in the species buoyancy force. The velocity distribution attains a distinctive maximum value in the vicinity of the plate and then decreases properly to approach the free stream value. It is noticed that the velocity increases with increasing values of Modified Grashof number (Gc).

Figure (3) depicts the effect of Prandtl number on complex velocity profiles in presence of foreign species such as Mercury ($Pr = 0.025$), Air ($Pr = 0.71$), Water ($Pr = 7.00$) and Methanol ($Pr = 11.62$) are shown in figure 3. We observe that from figure 3, the complex velocity decreases with increasing of Prandtl number $P(r)$. The effects of the thermal radiation parameter (N) on the complex velocity and temperature profiles in the boundary layer are illustrated in figures (4) and (8) respectively. Increasing the thermal radiation parameter (N) produces significant increase in the thermal condition of the fluid and its thermal boundary layer. This increase in the fluid temperature induces more flow in the boundary layer causing the velocity of the fluid there to increase. The nature of complex velocity profiles in presence of foreign species such as Hydrogen ($Sc = 0.22$), Helium ($Sc = 0.30$), Oxygen ($Sc = 0.60$) and Water vapour ($Sc = 0.66$) are shown in figure (5). The flow field suffers a decrease in complex velocity at all points in presence of heavier diffusing species. Figure (7) depicts that the temperature profiles (θ) against y taking different values of Prandtl number (Pr). The thermal boundary layer thickness is greater for fluids with small Prandtl number. The reason is that smaller values of Prandtl number are equivalent to increasing thermal conductivity and therefore heat is able to diffuse away from the heated surface more rapidly than for higher values of (Pr) .

Figure (9) shows the concentration field due to variation in Schmidt number (Sc) for the gasses Hydrogen, Helium, Water vapour and Oxygen. It is observed that concentration field is steadily for Hydrogen and falls rapidly for Water vapour and Oxygen in comparison to Helium. Thus Hydrogen can be used for maintaining effective concentration field and Helium can be used for maintaining normal concentration field. Figures (6) and (10) display the effects of the chemical reaction parameter (k_r) on the complex velocity and concentration profiles, respectively. As expected, the presence of the chemical reaction significantly affects the concentration profiles as well as the velocity profiles. It should be mentioned that the studied case is for a destructive chemical reaction (k_r). In fact, as chemical reaction (k_r) increases, the considerable reduction in the velocity profiles is predicted, and the presence of the peak indicates that the maximum value of the velocity occurs in the body of the fluid close to the surface but not at the surface. Also, with an increase in the chemical reaction parameter, the concentration decreases. It is evident that the increase in the chemical reaction (k_r) significantly alters the concentration boundary layer thickness but does not alter the momentum boundary layers.

The profiles for skin friction (τ) due to complex velocity under the effects of Grashof number (Gr) Modified Grashof number (Gc) Schmidt number (Sc) Prandtl number (Pr) Thermal radiation parameter (N) and Chemical reaction ($k - r$) are presented in the table (1). We observe from the above table (1), the skin friction

(τ) due to complex velocity rises under the effects of Grashof number (Gr) Modified Grashof number (Gc) Thermal radiation parameter (N) And the skin friction (τ) due to complex velocity falls under the effects of Schmidt number (Sc), Prandtl number (Pr) Chemical reaction (k_r). The profiles for Nusselt number (Nu) due to temperature profile under the effect of Prandtl number is presented in table (3). We see from this table the Nusselt number (Nu) due to temperature profile falls under the effect of Prandtl number (Pr) and rises under the effect of Thermal radiation parameter (N). The profiles for Sherwood number (Sh) due to concentration profiles under the effect of Schmidt number (Sc) and Chemical reaction (k_r) are presented in the table (3). We see from this figure the Sherwood number (Sh) due to concentration profile decreases under the effects of Schmidt number (Sc) and Chemical reaction (k_r) In order to ascertain the accuracy of the numerical results, the present results are compared with the previous analytical results of Muthucumaraswamy and Ganesan [15] for $Gr = Gc = 1.0$, $Pr = 0.71$, $Sc = 0.22$ and $k_r = 1.0$ in table (2). They are found to be in an excellent agreement. (τ) is

G_r	G_c	Sc	Pr	N	k_r	τ
1.0	1.0	0.22	0.71	1.0	1.0	1.2265
2.0	1.0	0.22	0.71	1.0	1.0	2.0398
1.0	2.0	0.22	0.71	1.0	1.0	2.6398
1.0	1.0	0.30	0.71	1.0	1.0	1.1684
1.0	1.0	0.22	0.70	1.0	1.0	0.4307
1.0	1.0	0.22	0.71	2.0	1.0	1.4568
1.0	1.0	0.22	0.71	1.0	2.0	0.3602

TABLE 1. Skin - Friction Coefficient(τ)

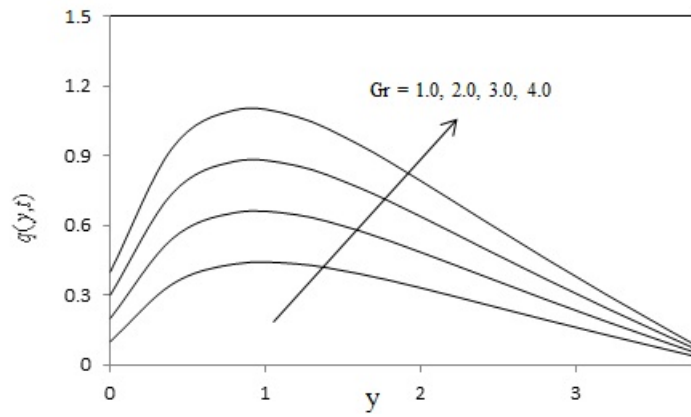
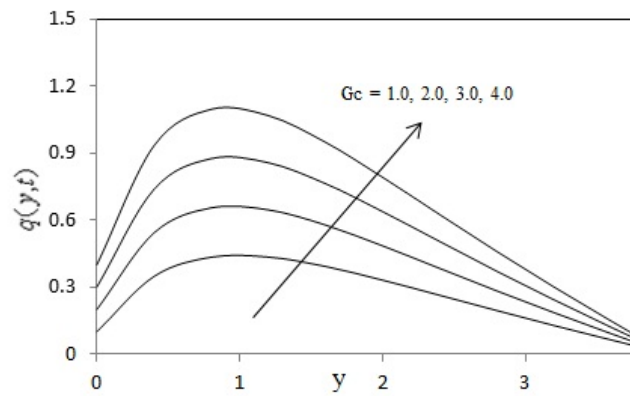
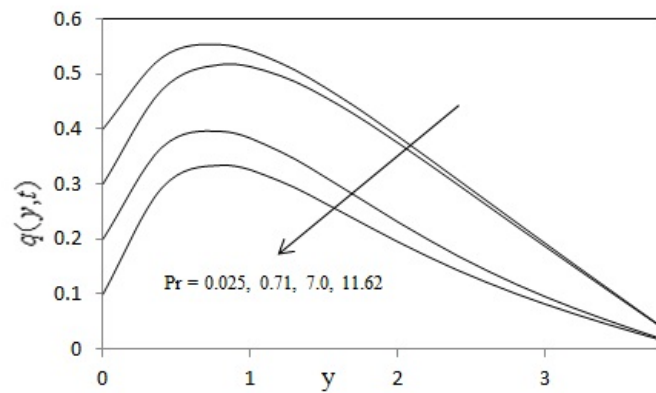
the Skin friction results obtained in the present study, and (τ^*) is Skin - Friction results obtained by Muthucumaraswamy and Ganesan [15]

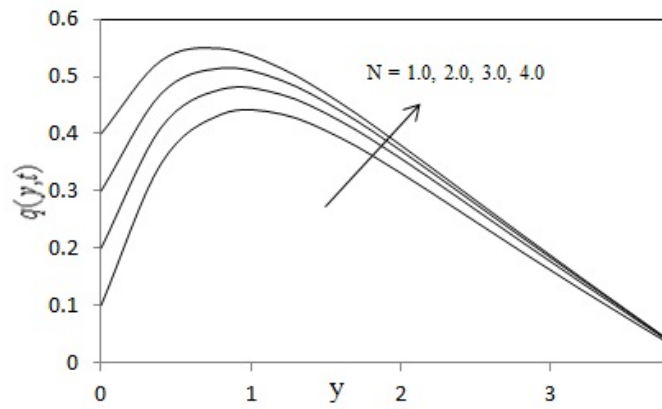
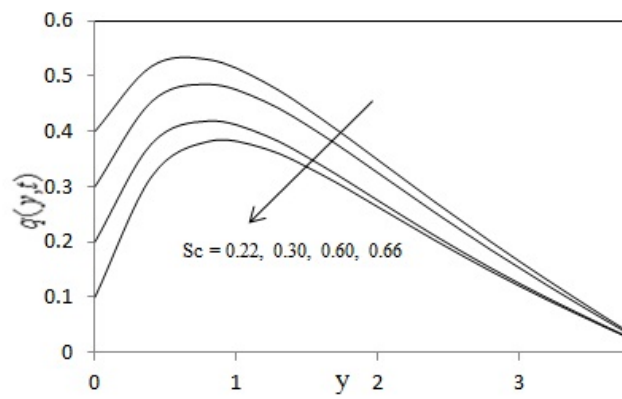
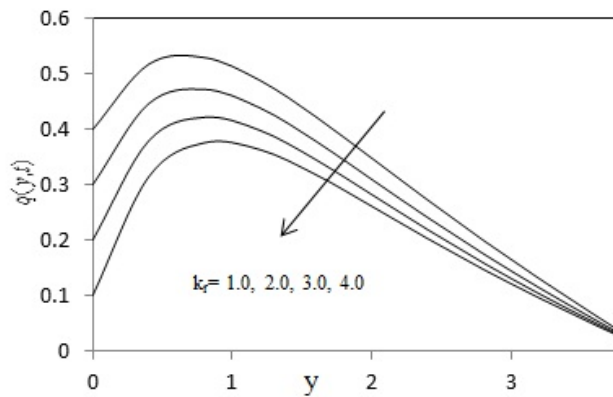
G_r	G_c	Sc	Pr	k_r	τ	τ^*
1.0	1.0	0.22	0.71	1.0	2.2265	2.2236
2.0	1.0	0.22	0.71	1.0	3.0398	3.0309
1.0	2.0	0.22	0.71	1.0	3.6398	3.6314
1.0	1.0	0.30	0.71	1.0	2.1684	2.1621
1.0	1.0	0.22	0.70	1.0	1.4307	1.4299
1.0	1.0	0.22	0.71	2.0	2.3602	2.3593

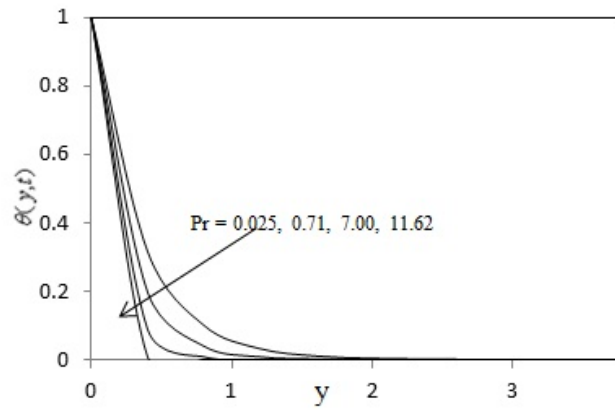
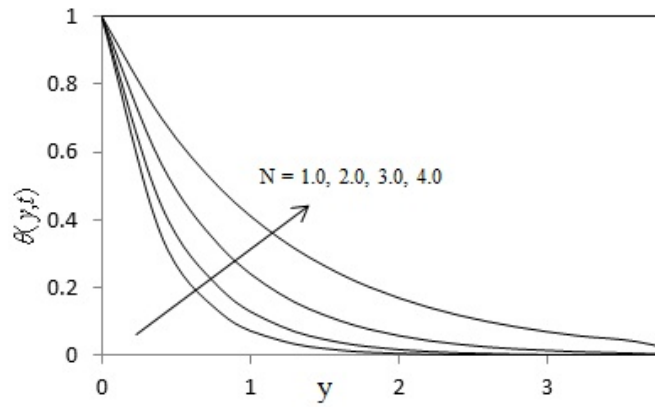
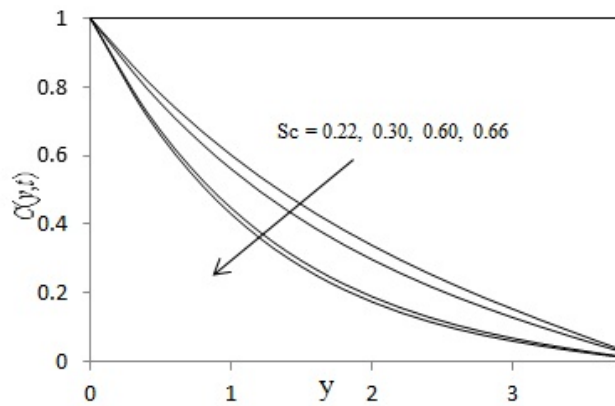
TABLE 2. Comparison between Skin - Friction (τ) and (τ^*)

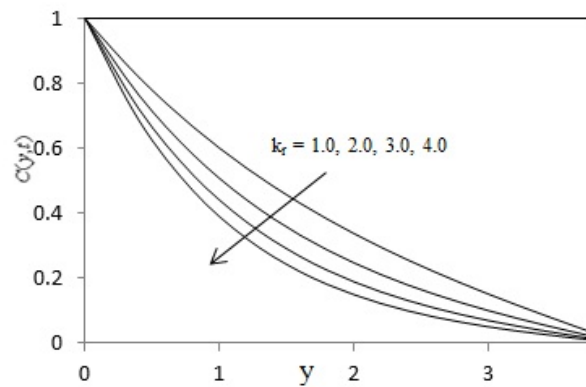
Pr	N	Nu	Sc	k_r	Sh
0.71	1.0	5.9361	0.22	1.0	7.3607
7.00	1.0	4.0179	0.71	1.0	7.1800
0.71	2.0	6.0335	0.22	2.0	7.2688

TABLE 3. Rate of heat and Mass transfer coefficients (Nu, Sh)

FIGURE 1. Velocity profiles for different values of Gr FIGURE 2. Velocity profiles for different values of Gc FIGURE 3. Velocity profiles for different values of Pr

FIGURE 4. Velocity profiles for different values of N FIGURE 5. Velocity profiles for different values of Sc FIGURE 6. Velocity profiles for different values of k_t

FIGURE 7. Temperature profiles for different values of Pr FIGURE 8. Temperature profiles for different values of N FIGURE 9. Concentration profiles for different values of Sc

FIGURE 10. Concentration profiles for different values of k_r .

5. CONCLUSION

In this study we have examined the governing equations for unsteady hydromagnetic natural convection heat and mass transfer flow of a rotating Boussinesq fluid past a vertical porous plate in the presence of radiative heat transfer. Employing Finite element technique, the leading equations are solved numerically in the complex plane. We present results to illustrate the flow characteristics for the velocity and temperature fields as well as the skinfriction, Nusselt number and Sherwood number show how the flow fields are influenced by the material parameters of the flow problem.

- (1) It is observed that the complex velocity (q) of the fluid increases with the increasing of parameters G_r, G_c, N and decreases with the increasing of parameters P_r, S_c and K_r .
- (2) The fluid temperature (θ) increases with the increasing of N and decreases with the increasing of P_r .
- (3) The Concentration of the fluid decreases with the increasing of K_r and S_c .
- (4) From table (1) it is concluded that the magnitude of shearing stress increases as the increasing values of G_r, G_c, N and this behavior is found just reverse with the increasing of P_r, S_c and K_r .
- (5) From table (3) it is concluded that the Nusselt number (Nu) increases as the increasing values of N and this behavior is found just reverse with the increasing of P_r .
- (6) From table (3) it is concluded that the Sherwood number (Sh) decreases as the increasing values of S_c and K_r . On comparing the skin friction τ results with the skin friction (τ^*) results of Muthucumaraswamy and Ganesan [15] it can be seen that they agree very well.

REFERENCES

- [1] Agrawal, H. L., P. C. Ram, V. Singh, Effects of Hall currents on the hydromagnetic free convection with mass transfer in a rotating fluid, *Astrophys. Space Sci.*, Vol. 100, pp. 279-283, 1984.

- [2] Azzam, G. E. A, Radiation effects on the MHD mixed free fixed convective flow past a semi infinite moving vertical plate for high temperature differences, Phys. Scripta., Vol. 66, pp. 71 76, 2002.
- [3] Bestman, A. R., and S. K. Adjepong, Unsteady hydromagnetic free convection flow with radiative heat transfer in a rotating fluid, Astrophys. Space Sci., Vol. 143, pp. 217 224, 1998.
- [4] Bestman, A. R., Free convection heat transfer to steady radiating non Newtonian MHD flow past a vertical porous plate, Int. J. Numer. Methods Eng., Vol. 21, pp. 899 908, 1985.
- [5] Chamkha, A. J., Thermal radiation and buoyancy effects on hydromagnetic flow over an accelerating permeable surface with heat source or sink, Int. J. Eng. Sci., Vol. 38, pp. 1699 1712, 2000.
- [6] Chamkha, A. J., Unsteady MHD convective heat and mass transfer past a semi infinite vertical permeable moving plate with heat absorption, Int. J. Eng. Sci., Vol. 42, pp. 217 230, 2004.
- [7] Cookey, C. I., A. Ogulu, V. B. Omubo Pepple, Influence of viscous dissipation and radiation on unsteady MHD free convection flow past an infinite heated vertical plate in a porous medium with time dependent suction, Int. J. Heat Mass Transfer, Vol. 46, pp. 2305 2311, 2003.
- [8] Elbarbary, E. M. E. and N. S. Elgazery, Chebyshev finite difference method for the effect of variable viscosity on magneto micro polar fluid flow with radiation, Mass Transfer Int. Comm. Heat, Vol. 31, No. 3, pp. 409 419, 2004.
- [9] Helmy, K. A., Unsteady free convection flow past a vertical porous plate, ZAMM. Z. Angew. Math. Mech., Vol. 78, No. 4, pp. 255 270, 1998.
- [10] Ibrahim, F. S., I. A. Hassanien, A. A. Bakr, Unsteady magnetohydrodynamic micro polar fluid flow and heat transfer over a vertical porous medium in the presence of thermal and mass diffusion with constant heat source, Canad. J. Phys., Vol. 82, pp. 775 790, 2004.
- [11] Jha, B. K., MHD free convection and mass transform flow through a porous medium, Astrophys. Space Sci., Vol. 175, pp. 283 289, 1991.
- [12] Kandasamy, R., K. Periasamy and K. K. S. Prabhu, Effects of chemical reaction, heat and mass transfer along a wedge with heat source and concentration in the presence of suction or injection, Int. J. Heat Mass Transfer, Vol. 48, pp. 1288 1394, 2005.
- [13] Muthucumaraswamy, R. and P. Ganesan, Natural convection on a moving isothermal vertical plate with chemical reaction, J. Eng. Phys. Thermophys., Vol. 75, No. 1, pp. 51 75, 2002.
- [14] Ogulu, A. and C. I. Cookey, MHD free convection and mass transfer flow with radiative heat transfer, Model. Measure. Contr. B, Vol. 70, No. 1 2, pp. 31 37, 2001.
- [15] Singh, A. K., N. C. Sacheti, Finite difference analysis of unsteady hydromagnetic free convection flow with constant heat flux, Astrophys. Space Sci., Vol. 150, pp. 303 308, 1988.

ASSISTANT PROFESSOR, DEPARTMENT OF BSH, BVRIT HYDERABAD COLLEGE OF ENGINEERING FOR WOMEN, BACHUPALLY, HYDERABAD - 500090, INDIA.

E-mail address: anithareddy1981@gmail.com